

ORIGINAL ARTICLE

Heterogeneous PdAg alloy catalyst for selective methylation of aromatic amines with formic acid under an additive-free and solvothermal one-pot condition

Ajay K Singh¹, Yoon-Ho Hwang¹ and Dong-Pyo Kim

The methylation of amines for the synthesis of methylamines and dimethylamines as platform chemicals has been attempted mostly by homogeneous catalysts with acid additives. However, there are scarcely any reports on heterogeneous catalytic methylation reactions except for a routine approach under high temperature and high pressure of CO₂ and H₂ gases for extended reaction times. Here we report a heterogeneously catalyzed selective methylation of aromatic amines using reactive and nontoxic formic acid as the only source for the construction of methyl groups, under ambient pressure in an additive-free one-pot reaction condition. Equal proportions of Pd and Ag in the PdAg/Fe₃O₄/N-rGO catalyst deliver highly selective amine methylation without aromatic ring hydrogenation, as the strained Pd in the alloy is combined with the graphene-derived support, preventing nanoparticle agglomeration and the action of magnetite as a promoter. Both *N*-methylation and *N,N*-dimethylation of various substituted aromatic amines were performed with complete conversion and excellent 90–97% selectivity by controlling the reaction times in the range of 10–24 h at 140 °C without unwanted aromatic ring hydrogenation. Furthermore, the developed bimetallic catalyst provided high yields (88–91%) of methylation with CO₂+H₂ gas under high pressure, which are as good as the results of homogenous catalysts with an acid additive. To the best of our knowledge, our use of this environmentally friendly methodology is the first time that this durable heterogeneous catalyst has readily performed highly selective methylation at ambient pressure, which is attractive for industrial applications.

NPG Asia Materials (2015) 7, e222; doi:10.1038/am.2015.116; published online 30 October 2015

INTRODUCTION

Amine methylation leads to the formation of methylamine,¹ dimethylamine² and formamide,³ which are used as platform chemicals for the synthesis of fertilizers, fungicides, synthetic leathers, and polymers and are directly used as solvents and formulation agents.³ The most common syntheses for the methylation of amines involve the use of methyl iodide,^{4,5} dimethyl sulfate,⁶ formaldehyde⁷ or diazomethane⁸ as methylating reagents with excellent reactivity. However, their toxicity and the stoichiometric generation of inorganic salt wastes raise environmental concerns. Therefore, the methylation of amines via environmentally acceptable reagents or routes is highly desirable. From this perspective, there have been various attempts at *N*-methylation by using a C₁-building block source (CO₂, formic acid) and/or a reductant (H₂, silanes and boranes) with organometallic catalysts, including rhodium, ruthenium and zinc complexes.^{1,3,9–14} However, these homogenous catalysts require challenging synthesis processes with an elaborately designed ligand complex, which is difficult to separate and recycle from the products.¹⁵ Furthermore, additives such as organic acids are needed for good performance, and high pressure and/or temperature are required.

Formic acid (FA), a biomass derivative, has attracted a great deal of attention as a suitable liquid for hydrogen production as an energy source and for hydrogenation reactions.¹⁶ It is potentially an excellent C₁ and hydrogen source for the methylation of amines, due to its nontoxicity, biodegradability and good reactivity with amines. Cantat *et al.* have used FA for an amine methylation reaction with a homogeneous Ru(COD)(methylallyl)₂ catalyst and two additives.¹⁰ Recently, Beller's group has reported aniline methylation via FA and hydrosilane with homogenous [Pt] Karstedt's catalyst and toxic organophosphorus ligand.¹⁷ For heterogeneous catalysts, Shimizu *et al.*¹⁸ have previously reported secondary amine methylation using a Pt-based heterogeneous catalyst under CO₂ and H₂ gas-phase conditions, but the drawbacks of that system were its rather harsh conditions, such as high temperature (over 200 °C), long reaction time (24 h) and high pressure (50 bar). However, it is surprising that there is no report on heterogeneous catalytic methylation reactions using FA as a building block without aromatic ring reduction, despite its obvious merits.

In this work, we report the heterogeneously catalyzed selective *N*-methylation and *N,N*-dimethylation of aromatic amines using FA as

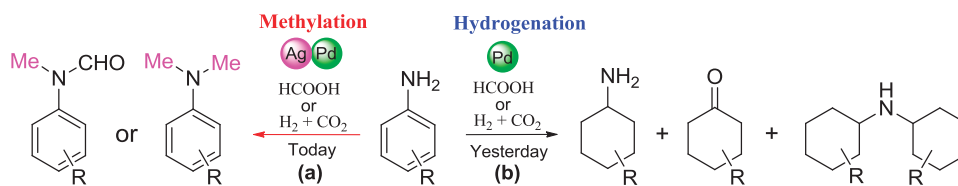
Department of Chemical Engineering, National Center of Applied Microfluidic Chemistry, POSTECH (Pohang University of Science & Technology), Pohang, Korea

¹These authors contributed equally to this work.

Correspondence: Professor D-P Kim Department of Chemical Engineering, National Center of Applied Microfluidic Chemistry, POSTECH (Pohang University of Science & Technology), Bldg., San31, Hyoja-dong, Pohang, 790-784, Korea.

E-mail: dpkim@postech.ac.kr

Received 3 May 2015; revised 13 July 2015; accepted 30 July 2015



Scheme 1 Comparative strategies for aromatic amine methylation. (a) Bimetallic catalyst for selective methylation of amine groups without benzene hydrogenation. (b) Known methods for hydrogenation of aniline using formic acid or (H₂+CO₂) with Pd-based catalyst.^{19–25}

Table 1 Methylation of aniline as a model reaction under an additive-free and solvothermal one-pot condition

Entry	Catalyst	Yield (%) ^a					
		2	3	4	5	6	7
1 ^b	Pd/N-rGO	86	5	7	0	0	0
2 ^b	Pd/C	95	0	3	0	0	0
3 ^c	Pd ₄₉ Co ₅₁ /N-rGO	0	0	0	22	0	0
4 ^c	Pd ₅₂ Au ₄₈ /N-rGO	0	0	36	12	0	0
5 ^c	Pd ₅₂ Pt ₄₈ /N-rGO	0	0	10	15	0	0
6 ^c	Pd ₄₈ Sn ₅₂ /N-rGO	0	0	0	70	0	0
7 ^c	Pd ₄₉ Ni ₅₁ /N-rGO	0	0	0	18	0	0
8 ^c	Pd ₄₈ Ag ₅₂ /N-rGO	0	0	0	86	3	0
9 ^c	Pd ₄₇ Ag ₅₃ /#	0	0	0	92	2	5
10 ^c	Pd ₃₁ Ag ₃₅ Co ₃₄ /#	0	0	0	80	0	0
11 ^c	Ag@Pd/C ²⁰	60	5	8	26	0	0

Reaction conditions: aniline (0.1 mmol), DCM (2 ml), formic acid (30 equivalent) at 140 °C for 10 h.

^aYield was determined by GC using n-hexadecane as an internal standard; complete conversion for all cases.

^bMetal catalyst (1.2 mol%).

^cPd 1.2 mol%; # = Fe₃O₄/N-rGO.

the only source for the construction of methyl groups under ambient pressure in an additive-free one-pot reaction. Of the various Pd-based bimetallic catalysts, a Pd₄₇Ag₅₃ alloy combination resulting from the introduction of an inactive Ag moiety showed synergistic catalytic activity in the methylation of both aniline and substituted anilines under solvothermal conditions at 140 °C. With no ring hydrogenation, highly selective monomethylation in 90–96% yield was achieved after continuing the reaction for 10 h, and dimethylation products in 90–97% yield were obtained by extending the reaction to 24 h in the presence of 30 equivalents of FA. Furthermore, high selectivity of the catalyst was retained with no leaching through up to five recyclings via simple filtration/centrifugation with loaded magnetic nanoparticles (NPs). In addition, the catalytic superiority was demonstrated by the nearly complete dimethylation of anilines with high selectivity (88–91%) under high pressures of CO₂ and H₂ gas mixtures in a sealed autoclave, which is comparable to the homogenous catalytic activity with the use of a strong acid additive. To the best of our knowledge, this methodology is the first case in which a durable heterogeneous catalyst readily performs highly selective methylation at ambient pressure. Therefore, we anticipate that this work may contribute substantially to the utilization of waste carbon as working carbon.

MATERIALS AND METHODS

Graphite powder (20- μ m flake size), sulfuric acid (95–97%), hydrogen peroxide (30 wt%), potassium permanganate, hydrazine hydrate (65% in water, Sigma-Aldrich, Seoul, Korea), Pd(NO₃)₂, AgNO₃, HAuCl₄, CoCl₂·6H₂O, PtCl₂, FeCl₃, FeCl₂, SnCl₄, Ni(NO₃)₂·6H₂O, formic acid (>99%), formic acid-d₂ and all organic solvents and reagents were obtained from Sigma-Aldrich chemicals. Deionized water (18.2 mS conductivity) was used in all experiments.

Synthesis of Pd₄₇Ag₅₃/Fe₃O₄/N-rGO catalyst

First, 2.0 g graphene oxide was dispersed in 1000 ml water in a beaker and sonicated for 3 h. Then, a solution of FeCl₃ and FeCl₂ (FeCl₃ = 0.810 g per 25 ml and FeCl₂ = 0.316 g per 25 ml) was added dropwise at room temperature. An aqueous solution of AgNO₃ (0.5 mmol, in 25 ml water) was added to the colloidal solution and stirred for 10 min. An aqueous solution of Pd(NO₃)₂ (0.5 mmol, in 25 ml water) was then added to the metal-dispersed solution at room temperature, and the reaction mixture was further stirred for 3 h to complete the mixing. Ammonia solution was added to achieve a pH = 10. The temperature of the solution was increased to 90 °C, and 15 ml of hydrazine hydrate (65% in water) was added with constant stirring, resulting in a black solution. After rapid stirring for 12 h, the solution was cooled to room temperature. The black solution was filtered, washed with water and acetone several times, and finally dried in a vacuum at 120 °C for 24 h.

RESULTS AND DISCUSSION

The well-established monometallic Pd catalyst is known to dehydrogenate formic acid to form H_2 , CO_2 ^{19,20} but it also hydrogenates, leading to unwanted aromatic ring hydrogenation and the dimerization of aniline (Scheme 1b).^{21–25} The development of a new heterogeneous catalyst is therefore highly desirable for selective amine methylation without aromatic ring hydrogenation (Scheme 1a). The approach taken in developing the homogeneous catalysts for amine methylation was believed to provide a direction for the development of a heterogeneous catalyst. We noted that controlling several parameters, such as the steric and electronic features of ancillary ligands, led to good selectivity.^{1,26} In this light, we envisioned that incorporating a less active transition metal with the active Pd could be a way of tuning the surface composition and ratio, ultimately retaining the bi-functional catalytic advantage with moderate hydrogenative reduction capacity (Scheme 1a). For this purpose, a series of mono-, bi- and tri-metallic catalysts were synthesized (see ESI† Supplementary Tables S1–S3). Initially, a series of bimetallic catalysts were synthesized by alloying Pd with another transition metal, such as Co, Au, Pt, Sn, Ni or Ag. These alloy metal catalyst NPs were supported on N-doped graphene oxide (N-rGO) to enhance their homogeneous distribution through chemical interactions, which prevented agglomeration and

leaching, even during the recycling process.²⁷ Furthermore, magnetite (Fe_3O_4) NPs were loaded for easy separation and high-mixing efficiency. The catalytic performance was evaluated using the model reaction between aniline and formic acid under an additive-free and solvothermal one-pot condition (140 °C, 10 h), in comparison to mono- and tri-metallic catalysts (Table 1 and see ESI† Supplementary Table S4). Both monometallic Pd/N-rGO and commercial Pd/C catalysts produced a mixture of cyclohexanone and dicyclohexylamine via active hydrogenation, as expected (entries 1 and 2, Table 1), which was consistent with the reported results,^{21–25} while a metal-free carbocatalyst (GO and N-rGO)^{28,29} and mono-metals (Ag, Co, Au, Pt, Ni and Sn) loaded on N-rGO showed almost no catalytic effect (see ESI† entries 1–10, Supplementary Table S4). Positively, the Pd-based bimetallic nano-alloys with transition metals (Co, Au, Pt, Sn and Ni) produced *N*-methyl-*N*-phenylformamide (5) as a methylation product in a yield range of 18–70% (entries 3–7, Table 1).

The PdAg nano-alloys significantly increased the yield of the methylation product (5) up to 86% (entry 8, Table 1), indicating that Ag could have a role as an electronic promoter, as previously reported.²⁰ In particular, it was interesting that magnetite loaded on PdAg/N-rGO further increased the yield to 92% and enhanced the catalytic efficiency by producing *N,N*-dimethylaniline (entry 9, Table 1). The synergistic effect was elucidated by the presence of chemically absorbed formate species on the magnetite, as observed by attenuated total reflectance infrared (ATR-IR) spectroscopy (see ESI† Supplementary Figure S1: monodentate formate at 1620 cm^{-1} arising from $\nu(\text{OCO})$ stretching, bridging formate at 1362 and 1580 cm^{-1} from the symmetrical and asymmetrical modes of O-C-O stretching), which presumably migrated to the nearby PdAg particles to promote the methylation of aniline at the active catalytic sites. Note that no catalytic activity of the Fe_3O_4 particle itself or of Fe_3O_4 /N-rGO was confirmed (see ESI† entry 4, Supplementary Table S4). A trimetallic system that diluted the Pd metal by incorporating two less active metals did not improve the reaction efficiency (entry 10, Table 1). Encouraged by the modulated catalytic activity of the bimetallic nano-alloy in the competition of hydrogenation and methylation, we further investigated various compositions of the PdAg NPs in detail. Five different PdAg NPs ($Pd_{88}Ag_{12}$, $Pd_{75}Ag_{25}$, $Pd_{66}Ag_{34}$, $Pd_{56}Ag_{44}$ and $Pd_{47}Ag_{53}$) were synthesized by varying the molar ratios of the precursors $Pd(NO_3)_2/AgNO_3$, and we determined the composition by inductively coupled plasma-atomic emission spectroscopy (see ESI† Supplementary Table S3).

Figure 1 shows the comparative catalytic efficiency of various Pd-based catalysts in the model reaction between aniline and formic acid under an additive-free and solvothermal one-pot condition (140 °C, 10 h). In general, a lower Pd ratio results in higher methylation. The $Pd_{88}Ag_{12}$ NPs still dominated the benzene ring

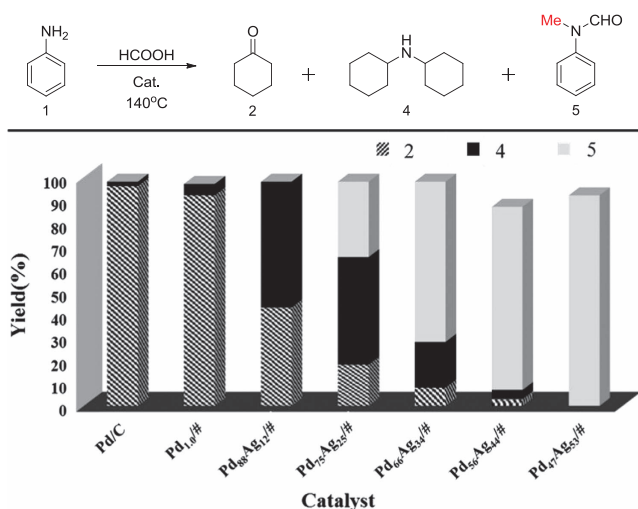


Figure 1 Competitive control of aniline hydrogenation and methylation by various PdAg catalysts under an additive-free and solvothermal one-pot condition. # = Fe_3O_4 /N-rGO. Reaction conditions: 140 °C for 10 h, 0.1 mmol aniline, catalyst (1.2 mol%, Pd), 30 equivalents formic acid, 2 ml DCM. Conversion and yields were determined via gas chromatography (GC) using *n*-hexadecane as an internal standard.

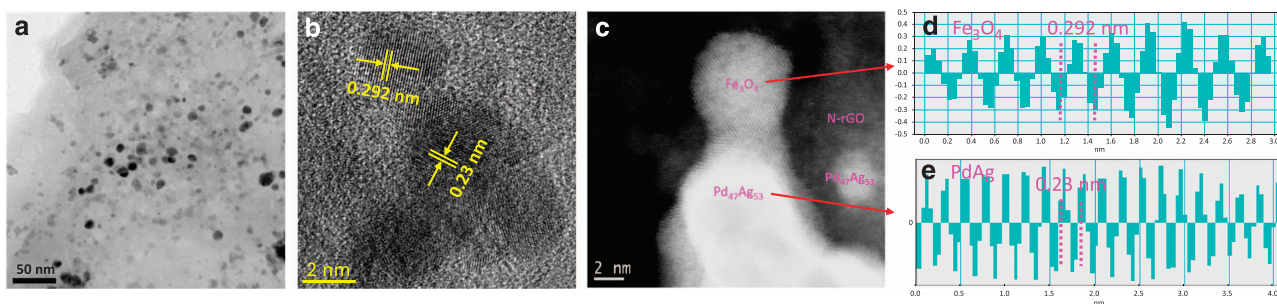


Figure 2 High-resolution transmission electron microscopic (HR-TEM) images with (a) low magnification and (b) high magnification; (c) dark field HAADF-STEM image of $Pd_{47}Ag_{53}/Fe_3O_4$ nanoparticles distributed on N-rGO supporter; (d and e) *d*-spacing line profiles of Fe_3O_4 and $Pd_{47}Ag_{53}$, respectively.

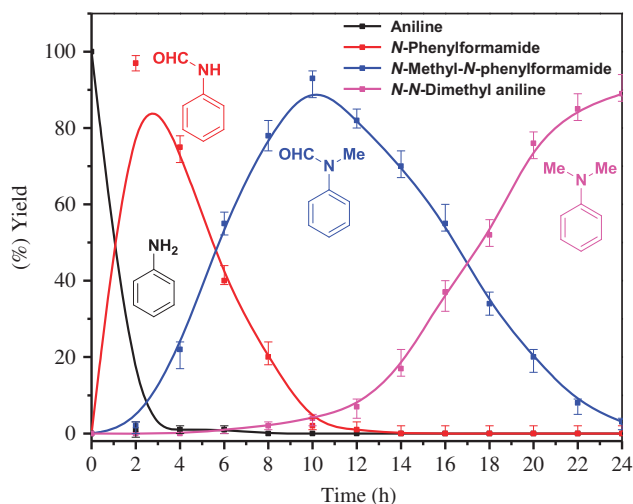


Figure 3 Time evolution of the N-methylation and *N,N*-dimethylation of aniline by Pd₄₇Ag₅₃ catalysts supported on Fe₃O₄/N-rGO. Reaction conditions: 140 °C, 0.1 mmol aniline, 1.2 mol% Pd, 30 equivalents formic acid, 2 ml DCM. Conversions and yields were determined by gas chromatography (GC), using *n*-hexadecane as an internal standard.

hydrogenation to produce a mixture of cyclohexanone (2) and dicyclo-hexylamine (4), and the Pd₇₅Ag₂₅ and Pd₆₆Ag₃₄ NPs began gradually increasing the methylation products. Eventually, the Pd₅₆Ag₄₄ and Pd₄₇Ag₅₃ catalysts, with further decreased Pd ratios, led to the prevailing formation of *N*-methyl-*N*-phenylformamide (5). In particular, it is worth noting that the superior catalytic activity of Pd₄₇Ag₅₃ relative to other combinations highlights the significant activity promotion resulting from the introduction of a catalytically inactive Ag moiety, which can be derived from the synergistic effects of metals. However, when the proportion of Pd in PdAg NPs is lower than 47%, the yield of the desired product (5) decreased, presumably due to the lesser availability of active surficial Pd metal.

To elucidate the reason for the markedly different catalytic activities of the Pd₄₇Ag₅₃ NPs on Fe₃O₄/N-rGO, the microstructure of the catalyst was first investigated via powered X-ray diffraction and transmission electron microscopy. When the Ag portion in PdAg NPs was increased, the diffused (111) peak shifted to a lower angle towards Ag (111), due to the increased lattice parameter, indicating that PdAg existed as an alloy rather than a two-metal phase (see ESI† Supplementary Figure S2b). Furthermore, the PdAg alloy NPs displayed uniform lattice patterns with no intraparticle boundaries, indicating a single alloyed phase with a (111) lattice fringe distance of 0.23 nm (Figure 2b and e) between the (111) lattice fringe distances of face-centered cubic Ag (0.24 nm) and face-centered cubic Pd (0.22 nm) NPs. The transmission electron microscopy image in Figure 2 shows that NPs with an average diameter of ~8 nm, consistent with X-ray diffraction measurements, were relatively dispersed on the N-rGO supporter without agglomeration (see ESI† Supplementary Table S6). Scanning electron microscope (SEM) and energy dispersive X-Ray spectroscopy (EDX) analysis further demonstrated the homogeneous distribution of all elements in the catalyst on the N-rGO surface (see ESI† Supplementary Figure S6). Magnetic Fe₃O₄ was also confirmed by characteristic X-ray diffraction peaks ($2\theta = 18.5^\circ, 30.1^\circ, 35.28^\circ, 43.2^\circ, 53.1^\circ, 57.48^\circ, 62.7^\circ$ and 74.0°) indexed to (111), (220), (311), (400), (422), (511), (440) and (533) as consistent with JCPDS No. 75-0033 (see ESI† Supplementary Figure S2a). In addition to high-resolution transmission electron microscopy (Figure 2c), atomic scale High angle annular dark field

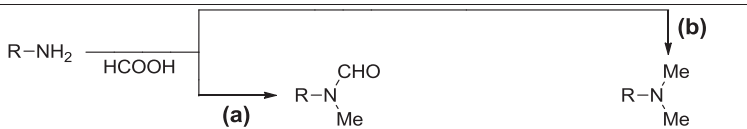
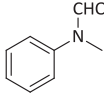
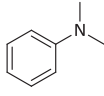
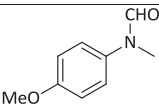
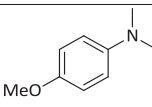
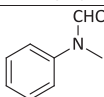
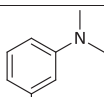
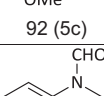
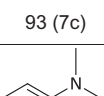
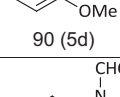
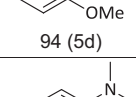
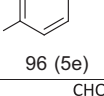
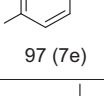
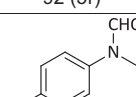
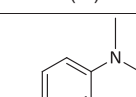
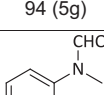
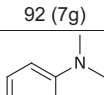
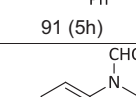
(HAADF)-scanning transmission electron microscopy (STEM) images with a probe correction and ~0.1-nm point resolution revealed the proximity between the PdAg particle (bright, ~8 nm) and the Fe₃O₄ particle (dark, 5~15 nm), with a 0.29 nm (400) lattice fringe (Figure 2a and d). Note that the intensity increased proportionally to the square of the atomic number of the elements.²⁶ Moreover, the surface chemistry of the multicomponent catalyst was determined by X-ray photoelectron spectroscopy (see ESI† Supplementary Figure S3). Doublet X-ray photoelectron spectroscopy peaks of Pd 3d (336 and 341 eV) and Ag 3d (368 and 374 eV) confirmed the metallic features of Pd⁰ and Ag⁰ (see ESI† Supplementary Figure S4e and S4f),³⁰ whereas the ratio of Pd/Ag (0.31 at %/0.33 at % = 0.94, Supplementary Table S5) in the surface composition was similar to the compositional Pd/Ag ratio (2.40 wt%/2.72 wt% = 0.89) measured by inductively coupled plasma-atomic emission spectroscopy, which is additional evidence of alloy structure. Three N1s peaks at ~399, 400 and 402 eV were assigned to the pyridinic, pyrrolic and graphitic or quaternary N (see ESI† Supplementary Figure S4c).^{28,29,31} The large amount of nitrogen (~4 at %) and oxygen atoms (~18 at %) in Supplementary Table S5 coordinated metal NPs on the graphene in a well dispersed and stable manner, preventing the re-oxidation of noble metal M⁰ (M = Ag, Pd), as reported for N-doped carbon.^{15,32} Therefore, a structural model of Pd₄₇Ag₅₃/Fe₃O₄/N-rGO could be hypothetically proposed (in ESI† Supplementary Scheme S1).

Importantly, the similarity in NP size between the PdAg nano-alloy and monometallic Pd indicates that the different catalytic activity is related to the alloying effect, rather than the size effect. It is well documented that a bimetallic alloy system would induce primary changes in not only the bond length due to the strain,³³ but also the bonding interactions of the surface heterometallic (Pd-M).³⁴⁻³⁸ To confirm the alloying effect, Ag cores and Pd shells were synthesized and dispersed in Vulcan carbon, as previously reported.^{20,39} When the prepared core-shell AgPd/C catalyst was employed in the model reaction between aniline and formic acid under solvothermal conditions, a mixture of hydrogenated products with a total yield of 73% was obtained (entry 11, Table 1). This result indicated that the existence of Ag atoms in the outermost layer (heterometallic Pd-Ag) was essential for avoiding over-hydrogenation. In particular, the Pd₄₇Ag₅₃ NPs alloy supported on Fe₃O₄/N-rGO was necessary for selective amine methylation reaction with preserved aromaticity, and these results demonstrated that elaborate modification of the catalyst surface at the atomic level and the consequent intermetallic electronic interaction would be an important pathway for controlling catalytic performance.³⁴

Assured of the catalytic feasibility of the PdAg nano-alloy for practical applications, we next investigated the solvent effects. Either dichloromethane or water was a good solvent to complete the conversion in the methylation of aromatic amine at 140 °C for 10 h, whereas DMSO, DMF, *o*-xylene, pyridine, toluene and benzene failed to produce the desired product in any appreciable yield (see ESI† Supplementary Table S7). Moreover, the time evolution of the reaction revealed that aniline was converted smoothly into *N*-methyl-*N*-phenylformamide and *N,N*-dimethylaniline without the unwanted formation of hydrogenated cyclohexanone (Figure 3). Highly selective monomethylation, with a 92% yield of methyl-*N*-phenylformamide, was achieved after continuing the reaction for 10 h at 140 °C, and a 96% yield of the dimethylation product, *N,N*-dimethylaniline, was obtained by extending the reaction to 24 h.

Interestingly, the reaction rate of the methylation depended on the amount of FA present (see ESI† Supplementary Figure S7). Thirty equivalents of FA produced the highest methylation yield, and this

Table 2 Selective *N*-methylation and *N,N*-dimethylation of various aniline derivatives by Pd₄₇Ag₅₃/Fe₃O₄/N-rGO catalyst

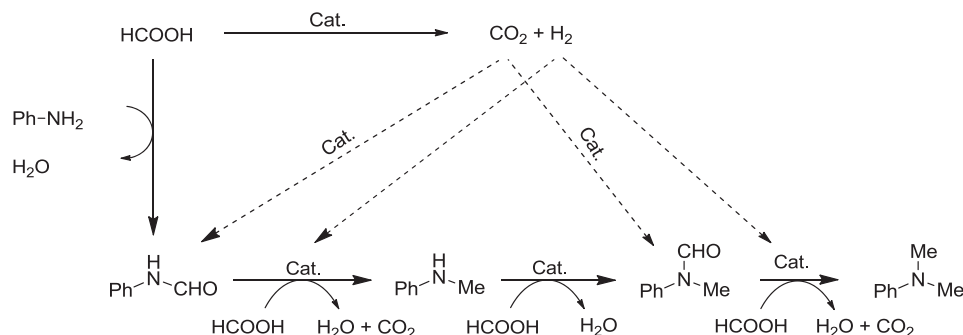
			
Entry	R	Yield 5 (%) ^c	Yield 7 (%) ^c
1	C ₆ H ₅	 92 (5a)	 96 (7a)
2	<i>p</i> -OMe-C ₆ H ₄	 94 (5b)	 97 (7b)
3	<i>m</i> -OMe-C ₆ H ₄	 92 (5c)	 93 (7c)
4	<i>o</i> -OMe-C ₆ H ₄	 90 (5d)	 94 (5d)
5	<i>p</i> -F-C ₆ H ₄	 96 (5e)	 97 (7e)
6	<i>m</i> -F-C ₆ H ₄	 92 (5f)	 93 (7f)
7	<i>p</i> -Ph-C ₆ H ₄	 94 (5g)	 92 (7g)
8	<i>o</i> -Ph-C ₆ H ₄	 91 (5h)	 90 (7h)
9	<i>p</i> -Cl-C ₆ H ₄	 90 (5i)	NA

Reaction conditions: substrates (0.1 mmol), catalyst Pd₄₇Ag₅₃/Fe₃O₄/N-rGO (1.2 mol%, Pd), formic acid (30 equiv.), DCM (2 ml). At least three measurements were taken to obtain average yields. In all cases, the complete conversion of aniline derivative was achieved.

^a140 °C, time 10 h.

^b140 °C, time 24 h.

^cyield is based on gas chromatography (GC) analysis using n-hexadecane (0.5 mmol) as an internal standard.



Scheme 2 Proposed pathways of Pd₄₇Ag₅₃-catalyzed methylation of anilines with formic acid and CO₂+H₂ gas.

condition was used throughout the reactions. With respect to practical applications, the catalyst should be highly stable, easily separable and readily recyclable without loss of activity. In the model reaction involving aniline methylation, the catalyst was recycled up to five times with no change in complete conversion but a small change in selectivity, from 92 to 86% (see ESI† Supplementary Table S8). When the catalyst was recycled five times, the surface ratio of Pd/Ag in the catalyst was slightly changed from the initial 0.94 of the Pd₄₇Ag₅₃ NPs with metals' synergistic effects to 1.04, according to X-ray photoelectron spectroscopy analysis (see ESI† Supplementary Table S5, and Supplementary Figure S5). Moreover, the magnetic NP-loaded catalyst could be easily separated from the reaction solution via simple filtration/centrifugation (see ESI† Supplementary Figure S8). When analyzed by inductively coupled plasma-atomic emission spectroscopy to check the possible leaching of metal NPs during the reaction, the concentrations of Ag and Pd in the reaction mixture were negligible at <0.1 p.p.m.

Next, the general scope of the supported Pd₄₇Ag₅₃ nano-alloy catalyst was extended by conducting the methylation of substituted anilines containing electron donation or withdrawal groups at different positions. As shown in Table 2, a variety of industrially relevant methyl formamides, such as methoxy-, phenyl- and fluorosubstituted *N*-methyl-*N*-phenylformamide, were prepared (route a) with excellent yields in the range of 90–96% after reacting for 10 h (Products 5a–5i). Subsequently, the substituted *N,N*-dimethylaniline products were also formed (route b) with high selectivity (90–97% yields) by simply extending the reaction time to 24 h (Products 7a–7h). To further enhance the synthetic profile of the one-pot solvothermal-methylation reactions, a scaled-up catalytic reaction of aniline (1) and formic acid was performed. Eventually, 2.0 g of isolated product (5a) with a 74% yield was obtained by an identical protocol with no use of additives, as previously described, indicating further upscaling potential (see ESI†, Section 3.3).

Furthermore, the alternative dimethylation of substituted anilines was performed using a mixture of CO₂ and H₂ gas under high pressure in a sealed autoclave with an identical catalyst (see ESI† Supplementary Table S9, route a). Surprisingly, the corresponding dimethylated anilines were produced with nearly complete conversion and excellent selectivity (88–92%) (see ESI† Supplementary Table S9, Products 7'a–7'h), which is similar to the reported activities of homogenous catalysts with the use of a strong acid additive.^{1,3,9–14} This unexpected conversion of anilines into *N,N*-dimethylanilines indicated the catalytic superiority of the heterogeneous Pd₄₇Ag₅₃ nano-alloy.

The reaction mechanism with formic acid as the alkylating reagent for the synthesis of *N*-methyl-*N*-phenylformamide and *N,N*-dimethylaniline was investigated by performing numerous

reactions with aniline and reaction intermediates (see ESI† Supplementary Figure S9). In the first step, Pd₄₇Ag₅₃ NPs exhibited superior catalytic dehydrogenation of FA, on the basis of an observation of TOF 497 h⁻¹ (see ESI† Supplementary Figure S10), which surpassed the previously reported values^{20,40,41} without forming CO byproducts, even at a higher temperature (90 °C; see ESI† Supplementary Figure S9, step 1).

A control reaction confirmed that methanol, produced from the excess of FA,⁴² is not a methylating agent, because very slow methylation of aniline occurred even at 140 °C for 10 h (see ESI† Supplementary Figure S9, step 2). A series of control reactions (see ESI† Supplementary Figure S9, steps 4–10) revealed that FA undergoes dehydrogenation during the earlier stages of methylation and in parallel serves as a formylation agent to yield the corresponding formamide in a competitive manner.

The subsequent methylation gradually proceeds with convergent reduction via transfer hydrogenation from HCOOH and the hydrogenation of H₂. It is well known that the methylation of the N–H bond with HCOOH involves the formation of formamide intermediates, which are reduced to an iminium species prior to the reduction to a N–CH₃ group.⁴³ Alternatively, a mixture of CO₂ as a C₁ source and H₂ as a direct reducing agent also partly contributed as a minor methylation route in this additive-free solvothermal condition, as previously reported.^{1,44} Finally, a plausible pathway is proposed in Scheme 2. To verify the origin of the incorporated hydrogen, an isotope-labeling experiment with d₂-formic acid was conducted to investigate the presence of hydrogen in the *N*-methyl-*N*-phenylformamide molecule (see ESI† Supplementary Figure S9, step 12). The detection of D-labeled *N*-methyl-*N*-phenylformamide (MW 139) without other protonated *N*-methyl-*N*-phenylformamides (MW 137, 138) clearly demonstrated that the FA is a main hydrogen source (see ESI† Supplementary Figure S11).

CONCLUSIONS

In summary, we have developed a novel heterogeneous catalyst for the methylation of aromatic amines with formic acid as a dual C₁-building block and reducing source via dehydrogenation, formylation and hydrogenation, which is the first described methylation reaction of amines in a solvothermal one-pot condition with no additives. The catalytic superiority of the heterogeneous Pd₄₇Ag₅₃ nano-alloy supported on Fe₃O₄/N-rGO correlated with the alloying effect that results when the inactive Ag atom is incorporated into the highly active Pd surface. Both the *N*-methylation and *N,N*-dimethylation of various substituted aromatic amines were performed with complete conversion and excellent selectivity in the range of 90–97% by controlling the reaction time in the range of 10–24 h. Furthermore, the bimetallic catalyst produced high yields (88–91%) in methylation with CO₂+H₂

gas under high pressure, which is as good as the results of homogenous catalysts with an acid additive. These results can provide valuable and practical methods for amine methylation.

CONFLICT OF INTEREST

The authors declare no conflicts of interest.

ACKNOWLEDGEMENTS

We gratefully acknowledge the support from a National Research Foundation (NRF) of Korea grant funded by the Korean government (MEST) (No. 2008-0061983).

- Li, Y., Sorribes, I., Yan, T., Junge, K. & Beller, M. Selective methylation of amines with carbon dioxide and H₂. *Angew. Chem. Int. Ed.* **52**, 12156–12160 (2013).
- Cui, X., Dai, X., Zhang, Y., Deng, Y. & Shi, F. Methylation of amines, nitrobenzenes and aromatic nitriles with carbon dioxide and molecular hydrogen. *Chem. Sci.* **5**, 649–655 (2014).
- Jacquet, O., Das Neves Gomes, C., Ephritikhine, M. & Cantat, T. Recycling of carbon and silicon wastes: room temperature formylation of N–H bonds using carbon dioxide and polymethylhydrosiloxane. *J. Am. Chem. Soc.* **134**, 2934–2937 (2012).
- Cardullo, F., Donati, D., Fusillo, V., Merlo, G., Paio, A., Salaris, M., Solinas, A. & Taddei, M. Parallel protocol for the selective methylation and alkylation of primary amines. *J. Comb. Chem.* **8**, 834–840 (2006).
- Chiappe, C., Piccioli, P. & Pieraccini, D. Selective N-alkylation of anilines in ionic liquids. *Green Chem.* **8**, 277–281 (2006).
- Onaka, M., Ishikawa, K. & Izumi, Y. Selective N-monoalkylation of aniline over alkali cation exchanged x and y type zeolites. *Chem. Lett.* **11**, 1783–1786 (1982).
- Byun, E., Hong, B., De Castro, K. A., Lim, M. & Rhee, H. One-pot reductive mono-alkylation of aniline and nitroarene derivatives using aldehydes. *J. Org. Chem.* **72**, 9815–9817 (2007).
- Iranpoor, N., Firouzabadi, H., Nowrouzi, N. & Khalili, D. Selective mono- and di-N-alkylation of aromatic amines with alcohols and acylation of aromatic amines using Ph₃P/DDQ. *Tetrahedron* **65**, 3893–3899 (2009).
- Jacquet, O., Frogneux, X., Das Neves Gomes, C. & Cantat, T. CO₂ as a C₁-building block for the catalytic methylation of amines. *Chem. Sci.* **4**, 2127–2131 (2013).
- Savourey, S., Lefevre, G., Berthet, J.-C. & Cantat, T. Catalytic methylation of aromatic amines with formic acid as the unique carbon and hydrogen source. *Chem. Commun.* **50**, 14033–14036 (2014).
- Tlili, A., Frogneux, X., Blondiaux, E. & Cantat, T. Creating added value with a waste: methylation of amines with CO₂ and H₂. *Angew. Chem. Int. Ed.* **53**, 2543–2545 (2014).
- Tlili, A., Blondiaux, E., Frogneux, X. & Cantat, T. Reductive functionalization of CO₂ with amines: an entry to formamide, formamidine and methylamine derivatives. *Green Chem.* **17**, 157–168 (2015).
- Blondiaux, E., Pouessel, J. & Cantat, T. Carbon dioxide reduction to methylamines under metal-free conditions. *Angew. Chem. Int. Ed.* **53**, 12186–12190 (2014).
- Das, S., Addis, D., Zhou, S., Junge, K. & Beller, M. Zinc-catalyzed reduction of amides: unprecedented selectivity and functional group tolerance. *J. Am. Chem. Soc.* **132**, 1770–1771 (2010).
- Jagadeesh, R. V., Surkus, A.-E., Junge, H., Pohl, M.-M., Radnik, J., Rabeah, J., Huan, H., Schünemann, V., Brückner, A. & Beller, M. Nanoscale Fe₂O₃-based catalysts for selective hydrogenation of nitroarenes to anilines. *Science* **342**, 1073–1076 (2013).
- Aresta, M., Dibenedetto, A. & Angelini, A. Catalysis for the valorization of exhaust carbon: from CO₂ to chemicals, materials, and fuels. technological use of CO₂. *Chem. Rev.* (2013).
- Sorribes, I., Junge, K. & Beller, M. General Catalytic Methylation of Amines with Formic Acid under Mild Reaction Conditions. *Chem. Eur. J.* **20**, 7878–7883 (2014).
- Kon, K., Siddiki, S. M. A. H., Onodera, W. & Shimizu, K.-i. Sustainable Heterogeneous Platinum Catalyst for Direct Methylation of Secondary Amines by Carbon Dioxide and Hydrogen. *Chem. Eur. J.* **20**, 6264–6267 (2014).
- Zhang, S., Metin, Ö., Su, D. & Sun, S. Monodisperse AgPd Alloy nanoparticles and their superior catalysis for the dehydrogenation of formic acid. *Angew. Chem. Int. Ed.* **52**, 3681–3684 (2013).
- Tedsree, K., Li, T., Jones, S., Chan, C. W. A., Yu, K. M. K., Bagot, P. A. J., Marquis, E. A., Smith, G. D. W. & Tsang, S. C. E. Hydrogen production from formic acid decomposition at room temperature using a Ag-Pd core-shell nanocatalyst. *Nat. Nanotechnol.* **6**, 302–307 (2011).
- Alper, H. & Vampollo, G. Catalytic reduction of the arene ring, and other functionalities, of organic substrates using formic acid and palladium on carbon. *Tetrahedron Lett.* **33**, 7477–7480 (1992).
- Orlova, S. T., Stromnova, T. A., Kazyul'kin, D. N., Boganova, L. I., Kochubey, D. I. & Novgorodov, B. N. Reactions of nitrosoarenes containing electron-withdrawing substituents with coordinated CO. Synthesis and structure of complexes Pd₂(OAc)₂(p-CIC₆H₄N[p-CIC₆H₃NO])₂ and Pd₂(OAc)₂(o-CIC₆H₄N[o-CIC₆H₃NO])₂. *Russ. Chem. Bull.* **53**, 819–824 (2004).
- Chatterjee, M., Sato, M., Kawanami, H., Ishizaka, T., Yokoyama, T. & Suzuki, T. Hydrogenation of aniline to cyclohexylamine in supercritical carbon dioxide: significance of phase behaviour. *Appl. Catal., A* **396**, 186–193 (2011).
- Rubio-Marques, P., Hernandez-Garrido, J. C., Leyva-Perez, A. & Corma, A. One pot synthesis of cyclohexanone oxime from nitrobenzene using a bifunctional catalyst. *Chem. Commun.* **50**, 1645–1647 (2014).
- Krishnankutty, N. & Vannice, M. A. The effect of pretreatment on Pd/C Catalysts: II. Catalytic Behavior. *J. Catal.* **155**, 327–335 (1995).
- Gross, E., LiuJack, H.-C., Toste, F. D. & Somorjai, G. A. Control of selectivity in heterogeneous catalysis by tuning nanoparticle properties and reactor residence time. *Nat. Chem.* **4**, 947–952 (2012).
- Scheuermann, G. M., Rumi, L., Steurer, P., Bannwarth, W. & Mülhaupt, R. Palladium nanoparticles on graphite oxide and its functionalized graphene derivatives as highly active catalysts for the Suzuki–Miyaura coupling reaction. *J. Am. Chem. Soc.* **131**, 8262–8270 (2009).
- Singh, A. K., Basavaraju, K. C., Sharma, S., Jang, S., Park, C. P. & Kim, D.-P. Eco-efficient preparation of a N-doped graphene equivalent and its application to metal free selective oxidation reaction. *Green Chem.* **16**, 3024–3030 (2014).
- Gao, Y., Hu, G., Zhong, J., Shi, Z., Zhu, Y., Su, D. S., Wang, J., Bao, X. & Ma, D. Nitrogen-doped sp²-hybridized carbon as a superior catalyst for selective oxidation. *Angew. Chem. Int. Ed.* **52**, 2109–2113 (2013).
- Sanyal, U., Davis, D. T. & Jagirdar, B. R. Bimetallic core-shell nanocomposites using weak reducing agent and their transformation to alloy nanostructures. *Dalton Trans.* **42**, 7147–7157 (2013).
- Park, S., Hu, Y., Hwang, J. O., Lee, E.-S., Casabianca, L. B., Cai, W., Potts, J. R., Ha, H.-W., Chen, S., Oh, J., Kim, S. O., Kim, Y.-H., Ishii, Y. & Ruoff, R. S. Chemical structures of hydrazine-treated graphene oxide and generation of aromatic nitrogen doping. *Nat. Commun.* **3**, 638 (2012).
- Xu, X., Li, Y., Gong, Y., Zhang, P., Li, H. & Wang, Y. Synthesis of palladium nanoparticles supported on mesoporous N-doped carbon and their catalytic ability for biofuel upgrade. *J. Am. Chem. Soc.* **134**, 16987–16990 (2012).
- Shan, S., Petkov, V., Yang, L., Luo, J., Joseph, P., Mayzel, D., Prasai, B. & Wang, L. Atomic-structural synergy for catalytic CO oxidation over palladium–nickel nanoalloys. *J. Am. Chem. Soc.* **136**, 7140–7151 (2014).
- Gao, F. & Goodman, D. W. Pd–Au bimetallic catalysts: understanding alloy effects from planar models and (supported) nanoparticles. *Chem. Soc. Rev.* **41**, 8009–8020 (2012).
- Sankar, M., Dimitrats, N., Miedziak, P. J., Wells, P. P., Kiely, C. J. & Hutchings, G. J. Designing bimetallic catalysts for a green and sustainable future. *Chem. Soc. Rev.* **41**, 8099–8139 (2012).
- Yin, Z., Lin, L. & Ma, D. Construction of Pd-based nanocatalysts for fuel cells: opportunities and challenges. *Catal. Sci. Technol.* **4**, 4116–4128 (2014).
- Yin, Z., Zhang, Y., Chen, K., Li, J., Li, W., Tang, P., Zhao, H., Zhu, Q., Bao, X. & Ma, D. Monodispersed bimetallic PdAg nanoparticles with twinned structures: formation and enhancement for the methanol oxidation. *Sci. Rep.* **4**, 4288 (2014).
- Yin, Z., Zhou, W., Gao, Y., Ma, D., Kiely, C. J. & Bao, X. Electrochemical oxidation of methanol. *Chem. Eur. J.* **18**, 4887–4893 (2012).
- Jones, S., Tedsree, K., Sawangphruk, M., Foord, J. S., Fisher, J., Thompssett, D. & Tsang, S. C. E. Promotion of direct methanol electro-oxidation by Ru terraces on Pt by using a reversed spillover mechanism. *ChemCatChem* **2**, 1089–1095 (2010).
- Zhou, X., Huang, Y., Xing, W., Liu, C., Liao, J. & Lu, T. High-quality hydrogen from the catalyzed decomposition of formic acid by Pd–Au/C and Pd–Ag/C. *Chem. Commun. (Camb)* 3540–3542 (2008).
- Gu, X., Lu, Z.-H., Jiang, H.-L., Akita, T. & Xu, Q. Synergistic Catalysis of metal–organic framework-immobilized Au–Pd nanoparticles in dehydrogenation of formic acid for chemical hydrogen storage. *J. Am. Chem. Soc.* **133**, 11822–11825 (2011).
- Miller, A. J. M., Heinekey, D. M., Mayer, J. M. & Goldberg, K. I. Catalytic disproportionation of formic acid to generate methanol. *Angew. Chem. Int. Ed.* **52**, 3981–3984 (2013).
- Habibi, D., Nasrollahzadeh, M. & Sahebkhaki, H. Green synthesis of formamides using the Natrolite zeolite as a natural, efficient and recyclable catalyst. *J. Mol. Catal. A: Chem.* **378**, 148–155 (2013).
- Li, Y., Fang, X., Junge, K. & Beller, M. A general catalytic methylation of amines using carbon dioxide. *Angew. Chem. Int. Ed.* **52**, 9568–9571 (2013).



This work is licensed under a Creative Commons Attribution 4.0 International License. The images or other third party material in this article are included in the article's Creative Commons license, unless indicated otherwise in the credit line; if the material is not included under the Creative Commons license, users will need to obtain permission from the license holder to reproduce the material. To view a copy of this license, visit <http://creativecommons.org/licenses/by/4.0/>

Supplementary Information accompanies the paper on the NPG Asia Materials website (<http://www.nature.com/am>)